

Stabilizing the silicon fullerene Si₂₀ by thorium encapsulation

Abhishek Kumar Singh,¹ Vijay Kumar,^{1,2} and Yoshiyuki Kawazoe¹

¹*Institute for Materials Research, Tohoku University, Aoba-ku, Sendai 980-8577, Japan*

²*Dr. Vijay Kumar Foundation, 45 Bazaar Street, K. K. Nagar (West), Chennai 600 078, India*

(Received 24 September 2004; revised manuscript received 26 October 2004; published 29 March 2005)

We show using *ab initio* electronic structure calculations that the dodecahedral fullerene of silicon Si₂₀ is stabilized by thorium encapsulation. Thorium is found to be the only element in the Periodic Table that stabilizes this fullerene with icosahedral symmetry in the neutral state. The preference for *sp*³ bonding in silicon makes it an optimal cage with all pentagonal faces in contrast to carbon for which C₂₀ is difficult to stabilize. Similar to C₆₀, this is the highest symmetry cluster of silicon and should be abundant. It could lead to the possibilities of novel new phases and derivatives of silicon.

DOI: 10.1103/PhysRevB.71.115429

PACS number(s): 61.46.+w, 36.40.Cg, 73.22.-f

I. INTRODUCTION

Novel nanostructures of silicon are currently of great interest for discovering the components of future miniature devices. The perceived roadblock in Si miniaturization¹ has led to efforts on carbon-based nanostructures and molecules as alternate viable due to their stability. This may, however, require a completely new approach to devices. Therefore, exceptionally stable nanostructures of silicon are desirable that could be produced in macroscopic quantities size selectively. Both carbon and silicon are isoelectronic and have the same bulk diamond structure with *sp*³ bonding. However, at the nanoscale the two behave entirely differently. Carbon prefers cage shaped structures called fullerenes² with predominantly *sp*² bonding as it also has another allotrope, graphite while silicon cages are unstable. The discovery of the icosahedral C₆₀ fullerene² led to a new approach of making novel materials in which clusters play the role of atoms. Also a large variety of molecular derivatives have been formed. Much interest was aroused in stabilizing similar structures³⁻⁷ of silicon. However, no such species could be found in experiments.⁸ Here we demonstrate that encapsulation of one Th atom stabilizes Si₂₀ in the fullerene structure with perfect icosahedral (*I_h*) symmetry similar to C₆₀ making it the most stable metal encapsulated cage cluster of silicon.

The synthesis of the smallest fullerene C₂₀ has been attempted but it has been difficult⁹ as it has all pentagonal faces and the bonding becomes more *sp*³ like. On the other hand, this feature should make a dodecahedral Si₂₀ cage preferred. But the energetically unfavorable dangling bonds on this cage lead to reconstruction such that the lowest energy isomer of Si₂₀ is a prolate shaped structure^{10,11} in which two Si₁₀ closed packed magic clusters are fused together. The latter occur in high abundance in the mass spectra of elemental silicon clusters¹² but Si₂₀ is not magic. Also larger clusters of elemental silicon do not exhibit any strong magic behavior. They have fullerene-like structures^{10,13} with a core of silicon atoms inside.

Recently encapsulation of a metal atom has been shown¹⁴ to lead to cage structures with size selection. Silicon cages with 10–16 atoms can be formed¹⁴⁻¹⁶ by choosing an appropriate transition metal atom. The largest cage of silicon

known so far has 16 atoms in a fullerene-like structure (eight pentagons and two square) with a Zr or Hf atom at the center.¹⁴ On the other hand Ti doping leads to a Frank-Kasper (FK) tetrahedral isomer of Ti@Si₁₆ to be the most stable one. These structures are very compact due to strong interactions between the metal atom and the silicon cage. These predictions have been subsequently confirmed from experiments¹⁷ on anion clusters which show high abundances of 15 and 16 silicon atom clusters doped with one Ti atom while the other clusters are much less abundant. Most recently high abundance of neutral Ti@Si₁₆ has been obtained almost exclusively.¹⁸ It has confirmed the predicted strong magic behavior of this cluster and supported further the theoretical results that metal encapsulation is a novel approach for size selective mass production of silicon clusters.

There have been attempts to stabilize a dodecahedral Si₂₀ fullerene cage by doping of a Zr atom. However, this gets distorted¹⁴ as 20 Si atoms around a Zr atom are too many. We also tried doping with Hf, but the dodecahedral structure distorts again. In order to find the most appropriate dopant to stabilize Si₂₀, we noted that the highest occupied molecular orbital (HOMO) of the dodecahedral Si₂₀ cage is threefold degenerate and is occupied with only two electrons (see below). Accordingly an atom with an oxidation state of +4 is most appropriate to stabilize Si₂₀. Earlier efforts¹⁹ with a bigger metal atom with valency 4 such as Pb again led to distorted structures. Moreover, the embedding energy of Pb, defined as the energy gained in doping the metal atom in the empty cage, is quite small (≈ 2 eV),^{19,20} making it unlikely that Pb doped cluster would exist in high abundance. Among the bigger metal atoms such as lanthanides and actinides, Th is the only atom²¹ whose principal oxidation state is +4. Its atomic radius is 1.80 Å compared with about 1.60 Å for Zr or Hf. These factors make it attractive for the stabilization of the Si₂₀ cage. We also explored doping of Ce, Pr, Tb in the lanthanide series and Pa, U, and Pu atoms in the actinide series as these also have +4 oxidation state in some compounds. However, with the exception of Th, in each case the cage distorts or lowers its symmetry.

II. METHOD

We use *ab initio* projected augmented wave method^{22,23} and a plane wave basis set within the spin-polarized density

functional theory and the generalized gradient approximation²⁴ (GGA) for the exchange-correlation energy. The pseudopotentials are taken as implemented in the Vienna Ab Initio Simulation Package (VASP). For silicon, only the outer $3s^23p^2$ electrons are taken as valence. However, for the f electron dopants, the semicore s and p electrons are also taken as valence. The reliability of the pseudopotentials has been tested for bulk Si and Th. The calculated lattice parameters (5.46 and 5.05 Å) and cohesive energies (4.73 and 6.18 eV/atom) for Si and Th, respectively are in excellent agreement with the experimental values (5.43 and 5.08 Å) and (4.63 and 6.20 eV/atom). While transferability of such pseudopotentials for mixed systems is generally expected, we further checked the suitability of the pseudopotentials in the case of bulk α -Si₂Th which has the $I4_1/amd$ structure.²⁵ We use this as the starting structure and $8 \times 8 \times 3$ Monkhorst-Pack \mathbf{k} -point mesh for representing the Brillouin zone. The ionic positions and unit-cell volume as well as shape have been relaxed. The optimized structure remains the same and the calculated unit cell parameters are $a=b=4.140$ Å and $c=14.426$ Å as compared to the experimental values of $a=b=4.126$ Å and $c=14.346$ Å. The calculated cohesive energy for Si₂Th is 5.80 eV/atom and the heat of mixing is 1.77 eV per formula unit which is close to the experimental value²⁶ of 1.80 eV per formula unit. Thus our calculated lattice constants lie within 0.5% and the heat of mixing within 1.7% of the experimental values and show excellent agreement. We therefore trust the suitability of these potentials for the mixed systems as considered here. For clusters, the Brillouin zone is represented by the Γ -point. The conjugate gradient technique is used to optimize the structures without any symmetry constraints. As conjugate gradient technique leads to a local minimum, we considered a few structures as well as used random displacement of atoms for our search of lowest energy structure. The structures are considered to be converged when the force on each ion becomes 0.001 eV/Å or less. This high accuracy is also necessary to differentiate between closely lying structures that differ only by a small amount in the bond lengths that reduce the symmetry of the cluster.

III. RESULTS AND DISCUSSIONS

A. Stability of the I_h -Th@Si₂₀ fullerene

Three different initial structures are considered for Si₂₀Th: (i) a dodecahedral fullerene cage with Th at the center, (ii) the prolate shaped structure¹¹ of Si₂₀ with Th in between the two Si₁₀ clusters, and (iii) a 20-atom cage structure that is found in the bulk Ce₃Mg₄₂ phase.²⁵ The optimized fullerene structure [Fig. 1(a)] is the lowest in energy. The second best structure [Fig. 1(b)] is obtained from (iii) above and it lies 2.3 eV higher in energy. This large difference in energy and the I_h symmetry make the fullerene isomer very special. Its Si–Si bond length (2.35 Å) is almost the same as in bulk and the Si–Th bond length (3.29 Å) is only slightly longer than the calculated and experimental²⁵ values of, respectively, 3.164 and 3.16 Å in α -Si₂Th. This small increase is presumably due to the high coordination of Th atom in the dodecahedral cluster as compared to twelve (Si atoms) in α -Si₂Th.

The coordination of twenty is the highest among the known structures of silicon. The embedding energy (13.90 eV) of Th in the Si₂₀ cage is close to the highest value of 14.18 eV obtained¹⁴ for Hf in the Si₁₆ cage confirming that Th doping stabilizes the I_h cage with very strong bonding. This also leads to enhanced binding energy of 4.20 eV/atom in Th@Si₂₀ compared with 4.0 and 4.16 eV/atom for Si₂₀ and previously best fullerene-like structure of Zr@Si₁₆, respectively, making it one of the most stable metal encapsulated silicon clusters.

In order to find the optimal size of the silicon cage with Th doping, we doped Th in high symmetry 16- and 24-atom Si cages. For Th@Si₁₆ the fullerene-like isomer lies 1.42 eV lower in energy than the FK isomer. Th doping creates significant strain in the fullerene-like Si₁₆ cage as the Si–Si bond lengths (2.34, 2.37 and 2.49 Å) get elongated compared with the values of 2.29, 2.32, and 2.38 Å in Zr@Si₁₆¹⁴ and 2.35 Å in Th@Si₂₀ leading to lower binding (4.09 eV/atom) and embedding (11.80 eV) energies. Therefore, Si₁₆ cage is not optimal for Th doping. For Si₂₄ we considered the C₂₄ fullerene cage with Th at the center. Optimization of this cluster leads to the shrinkage of the cage such that three atoms pop out [Fig. 1(c)] showing that a cage with 24 Si atoms is too big for Th. These results suggest that Si₂₀ cage is more preferred. Finally we distort the I_h -Th@Si₂₀ cage with large random displacements of atoms in order to check if we are not trapped in a local minimum. The initial structure [Fig. 1(d)] has nearest neighbor Si–Si bond lengths in the range of 1.19 to around 3 Å while Si–Th bond lengths were in the range of 2.09 to 3.41 Å. However, upon optimization the structure remarkably comes back restoring the full I_h symmetry. The gain in energy from initial to the final configuration is 78.4 eV. It gives us confidence that the I_h -Si₂₀ cage is very stable and uniquely favorable in the case of silicon as C₆₀ is for carbon fullerenes with a wide basin of attraction in the energy-configuration space. The presence of all pentagonal faces on this cage provides the optimal bonding between the Si atoms similar to the preferred sp^3 type with minimal strain that is distributed uniformly over the whole cage, while the dangling bonds are pacified to a large extent by encapsulation of a Th atom due to strong covalent bonding (see below) between Th and the Si cage. Therefore, Th@Si₂₀ is the only cage of silicon to be of the lowest energy in this size range with I_h symmetry and stabilized by a metal atom. Hexagons in the silicon cage structures represent strain²⁷ like pentagons in carbon fullerenes and therefore Si₆₀ fullerene with 20 hexagons is not ideal for silicon.

B. Bonding nature and the electronic structure

The bonding nature has been studied from the total electronic charge density isosurfaces and the distribution of electronic states. In the case of I_h -Th@Si₂₀ and the corresponding empty Si₂₀ cage, Figs. 2(a) and 2(b) show covalent bonding between the Si atoms. There is a dip in the charge density isosurfaces at the centers of pentagons and the directional bonding is clearly seen. In this cage the bond angles in pentagons are very close to the tetrahedral angles and therefore the bonding between the Si–Si atoms can be considered

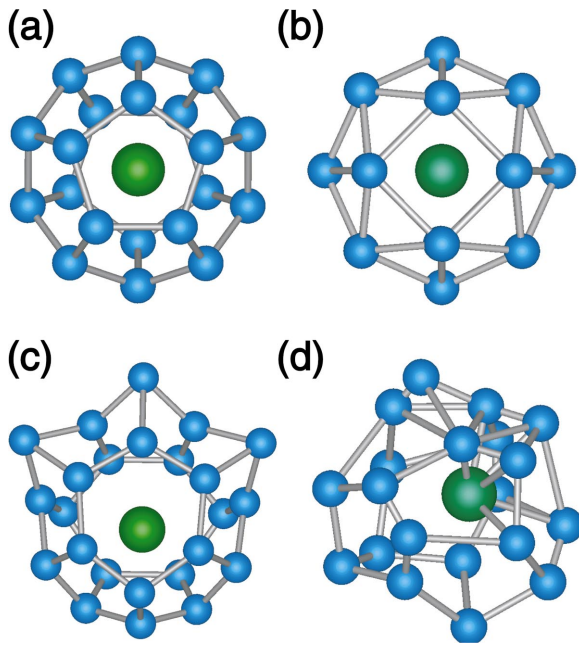


FIG. 1. (Color) Optimized structures of (a) I_h -Th@Si₂₀, (b) second best structure for Th@Si₂₀, (c) Th@Si₂₄, and (d) initial structure with large random displacements of atoms which converges back to the dodecahedral structure shown in (a). The metal atom (green) is inside the cage.

to be close to sp^3 with three lobes from each Si atom pointing towards three neighboring Si atoms that lead to the formation of strong σ bonds. The 4th lobe points outwards of the cage on each Si atom and leads to π bonded low density charge cloud outside of the cage. The difference in the electronic charge density of the I_h -Th@Si₂₀ [Fig. 2(a)] and the overlapping charge densities of Th and the empty I_h -Si₂₀ [Fig. 2(b)] cage with the same positions of atoms as in I_h -Th@Si₂₀ shows excess [Fig. 2(c)] of charge between the Th atom and the Si cage. Some of the charge from the Si-Si bonds as well as outside of the cage [Fig. 2(c)] is transferred inside the cage due to the covalent bonding between the orbitals of Th atom and of the Si cage (see below). This weakens the dangling bonds. This picture of the bonding nature is also reflected in the electronic states as well.

The electronic states of this fullerene are shown in Fig. 3 and these have been labeled according to the icosahedral symmetry. The HOMO and Lowest unoccupied molecular orbital (LUMO) states have the T_{2u} and G_u symmetries, respectively. In order to understand the bonding, the electronic structure, can also be described by a spherical model potential due to the high symmetry of the cage^{28,29} using an angular quantum number l and a principal quantum number n , reflecting the radial character of the wave functions. The states representing the three σ bonds for each Si in the dodecahedral Si₂₀ cage correspond to $n=1$ with 50 valence electrons accommodated in the $1s$, $1p$, $1d$, $1f$, and $1g$ states. The remaining 10 valence electrons occupy the $1h$ state partially. Under the icosahedral symmetry the $1h$ state splits into a fivefold degenerate state which is fully occupied and two threefold degenerate states which are empty. The remaining 20 electrons in π -bonded orbitals pointing outwards from the

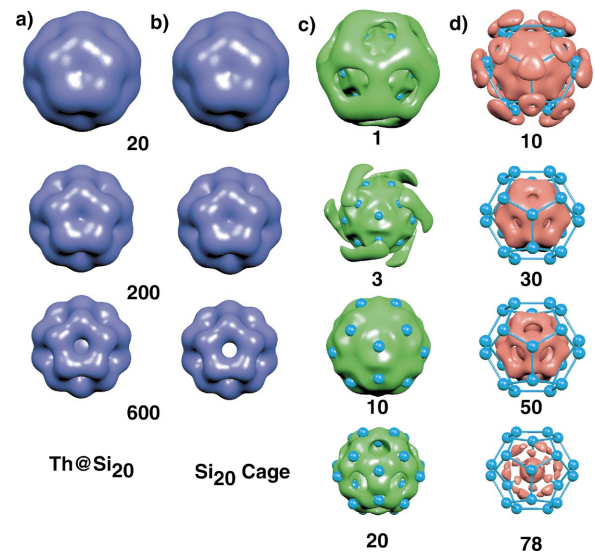


FIG. 2. (Color) Isosurfaces of the total electronic charge density, shown along the fivefold axis for different values of the density, for (a) I_h -Th@Si₂₀ fullerene and (b) I_h -Si₂₀ cage with the same atomic positions. (c) and (d) show the isosurfaces for the depletion and excess of charge shown along the threefold axis. The isosurfaces for different values of the density show the extent by which the charge is redistributed upon Th doping. The isosurfaces for the depletion of charge show removal of charge on the cage as well as outside of the cage. The depletion of charge outside of the cage is from the states with principle quantum number 2 in the spherical potential model. These dangling bond states are π bonded and depletion of charge shows weakening of the dangling bond states. Some charge is depleted just above the Si-Si bonds that is from the σ bonded states and it is pulled down slightly within the cage. The numbers below the figures indicate the value of the isosurface in the unit of $2.963 \times 10^{-4} e/\text{\AA}^3$. The depletion of charge in the isosurface corresponding to density 3 shows that there are two types of orbitals that are involved: one forming a cover on a pair of atoms which is stronger and the other on top of some atoms (this is seen more clearly for the lower value, 1, of the isosurface). Also the isosurface corresponding to 20 shows that significant charge is depleted from the top of the Si-Si bonds. The buildup of charge can be seen between the cage and the Th atom. There is high excess density along the Si-Si bonds but the maximum is between Si and Th atoms.

cage as discussed above occupy the $n=2$ states $2s$, $2p$, and $2d$ completely ($18 e$) and the $2f$ state partially ($2 e$). These states lie close to the HOMO as these are significantly less bound due to π bonding as compared to the σ bonded states on the cage. The calculated electronic structure of the I_h -Si₂₀ cage (Fig. 3) follows this scheme very closely. In the icosahedral symmetry, the $2f$ level splits into a threefold degenerate HOMO state, which is occupied by two electrons and an empty fourfold degenerate state. Thorium atom lies at the center of the cage and its orbitals hybridize strongly only with those orbitals of the Si₂₀ cage that have the same angular momentum character. With $7s^2 6d^2 5f^0$ valence electronic configuration of Th, the Th states lie above the HOMO of the Si cage as shown in Fig. 3 and interact with $1s$, $2s$, $1d$, and $2d$ states of the cage. This leads to a downward shift in the energies of these states while the $1f$ state remains nearly unchanged. The strongest hybridization occurs between the

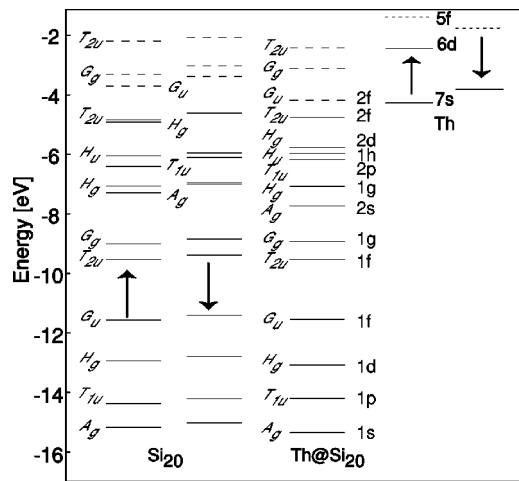


FIG. 3. The electronic states of the I_h -Th@Si₂₀ fullerene and the corresponding up- and down-spin states of the dodecahedral Si₂₀ empty cage and Th atom. The unoccupied states are shown by the broken lines. The states for the Si₂₀ cage and the I_h -Th@Si₂₀ fullerene are labeled with symmetries associated with the icosahedral group as well as using the principal and angular momentum quantum numbers for a spherical potential as described in the text. The states for the Th atom are labeled using the standard notation for atoms. These lie above the HOMO of the Si₂₀ cage. The 6d state of the Th atom and the threefold degenerate 2f state of the Si cage are occupied by only 2 electrons in each case. Note the shift in the energies of the cage states is most significant for the 2d states due to the strong hybridization with the Th 6d orbitals. For more details, see the text.

6d states of Th and the 2d states of the cage such that the bonding states are significantly pushed down (see in Fig. 3 that the H_g state of the Si₂₀ cage without Th atom around -4.5 eV shifts to around -5.49 eV after Th doping) while the antibonding states lie about 3.6 eV above the HOMO of the Th doped cage. This strong covalent bonding leads to a large gain in energy with Th doping.³⁰

The four valence electrons of thorium occupy the vacancies in the threefold degenerate hybridized 2f bonding states. The fourfold degenerate LUMO hybridizes more strongly with the 5f states of Th due to less energy separation and gets shifted downwards while the hybridized Th 5f states lie at around -2.15 (T_{2u}) and -1.43 eV (G_u). Most of the other states of the empty I_h -Si₂₀ cage are only weakly perturbed. The presence of the 2f complex in the HOMO and LUMO states makes the stability of the cage very sensitive to their occupancies. Thorium is ideal as the threefold degenerate 2f state is fully occupied while the 5f states of Th remain empty. It is one of the main reasons that the stabilization occurs with thorium. Doping with other actinide and lanthanide atoms³² and in particular Ce shows that the dodecahedral structure reduces to a cubic symmetry with Si-Si bond lengths of 2.33 and 2.37 Å. This makes thorium very special. The HOMO-LUMO gap of the I_h -Th@Si₂₀ fullerene is 0.58 eV. This is small compared with 1.58 eV for Zr@Si₁₆,¹⁴ due to the fact that in I_h -Th@Si₂₀ the gap arises due to the filling of a subshell in contrast to a shell for the Si₁₆ cage considering a spherical potential well. The true gap is, however, likely to be about 1 eV due to the underestimation by GGA.

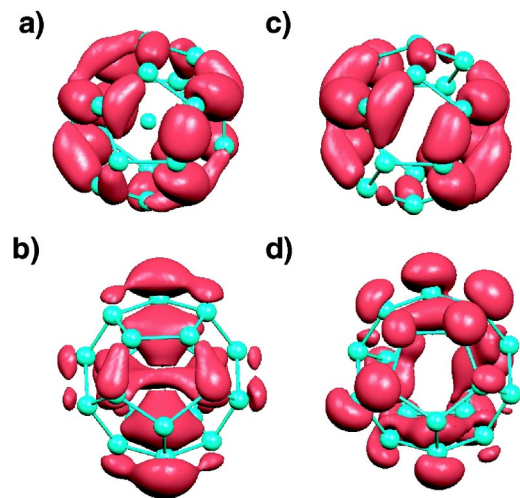


FIG. 4. (Color online) The partial electronic charge density isosurfaces of (a) one of the fivefold degenerate 1h type orbitals and (b) one of the fivefold degenerate 2d type orbitals for the Th@Si₂₀ fullerene. (c) and (d) show the corresponding partial charge density isosurfaces of the empty cage Si₂₀ orbitals. As compared to (b) the charge density in (d) lacks symmetry because of small differences in the occupation of the states due to smearing. In (b) the hybridization with the d orbitals of the Th atom is clearly seen, whereas the charge density from the h type orbitals changes little after Th doping. The isosurface value for all the cases is the same ($30 \times 2.963 \times 10^{-4} e/\text{Å}^3$).

The above discussion of the bonding as well as electronic structure is further corroborated from the electronic charge density distributions from the 1h, 2d, and 2f orbitals. Figure 4 shows the isosurfaces of the partial electronic charge densities from one of the 1h and 2d orbitals of the doped and empty Si cages. It is clearly seen that the charge density distribution in the 1h orbital is affected little by doping of the Th atom while the charge density distribution in the 2d orbital³¹ shows strong hybridization between the Si cage and the Th orbitals, consistent with the above description of the electronic spectrum. Furthermore Fig. 5 shows the isosurfaces of the charge density distribution for the HOMO and LUMO 2f states. The HOMO shows a weaker hybridization while the LUMO shows a stronger hybridization as discussed above.

As such clusters are potentially interesting for developing cluster assembled materials, we also studied interaction between two fullerenes. The structure with pentagons from two fullerenes facing each other in a prism configuration has the lowest energy. The cage structure is retained with the binding energy of 2.09 eV/fullerene that is much smaller than the value within a fullerene or pure silicon clusters¹⁰ of similar size. Further studies on a 3-dimensional packing of the fullerenes have been performed considering a cubic structure with relaxation of shape and volume of the unit cell. These results show that the cage structure is retained with the cubic symmetry. The binding energy per fullerene is 6.71 eV. Therefore, there is a potential for developing assemblies of this fullerene. Also it would be of interest to develop derivatives³³ of silicon fullerene as it has been achieved for carbon.

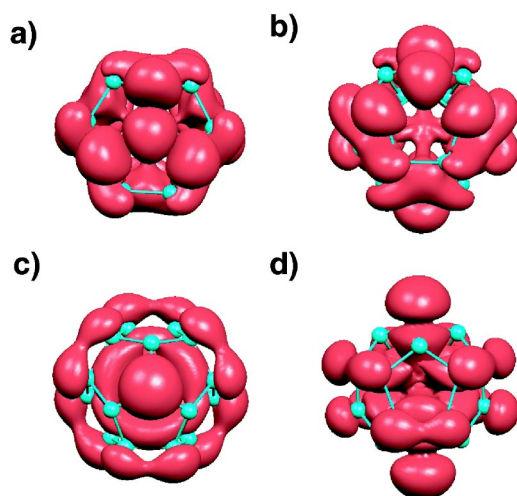


FIG. 5. (Color online) The partial charge density isosurfaces of (a) one of the threefold degenerate $2f$ type HOMO states and (c) one of the fourfold degenerate $2f$ type LUMO states viewed along the threefold axis of the fullerene. (b) and (d) represent, respectively, the charge density isosurfaces viewed along the fivefold axis. In the latter case charge density is clearly seen inside the cage. Also it shows that this density is small for the HOMO while much larger for the LUMO reflecting strong hybridization of the Th orbitals with the LUMO. The isosurface value for all the cases is the same ($10 \times 2.963 \times 10^{-4} e/\text{\AA}^3$).

IV. SUMMARY

In summary, we have shown that Th encapsulation stabilizes the highest symmetry fullerene cage of Si₂₀ with optimal bonding. In contrast to carbon for which pentagons represent strain in fullerenes, these are the most favored in silicon and therefore make Si₂₀ cage ideal. Accordingly we expect high abundances of I_h -Th@Si₂₀ fullerene. Our results also suggest that Th is the only atom which stabilizes this neutral fullerene with icosahedral symmetry. This is the largest Si cage that can be stabilized by doping of one metal atom. Therefore there is a strong selectivity in making this structure and it would be interesting to see this experimentally. Similar to C₆₀, we hope this finding will intensify research on the novel nanoforms of silicon, their various applications and functionalization.

ACKNOWLEDGMENTS

The authors would like to thank the staff of the Center for Computational Materials Science at the Institute for Materials Research for the use of the Hitachi SR8000/64 supercomputing facilities. A.K.S. is grateful for the support of MEXT and JSPS. V.K. is thankful for the hospitality at the Institute for Materials Research and for the partial support from the Asian office of Aerospace Research and Development.

- ¹M. Schulz, *Nature (London)* **399**, 729 (1999).
- ²H. W. Kroto, J. R. Heath, S. C. O'Brien, R. F. Curl, and R. E. Smalley, *Nature (London)* **318**, 162 (1985).
- ³M. Harada, S. Osawa, E. Osawa, and E. D. Jemmis, *Chem. Lett.* **1**, 1037 (1994).
- ⁴D. E. Jemmis, J. Leszczynski, and E. Osawa, *Fullerene Sci. Technol.* **6**, 271 (1998).
- ⁵E. F. Sheka, E. A. Nikitina, V. A. Zayets, and I. Y. Ginzburg, *Int. J. Quantum Chem.* **88**, 441 (2002).
- ⁶H. Tanaka, S. Osawa, J. Onoe, and K. Takeuchi, *J. Phys. Chem. B* **103**, 5939 (1999).
- ⁷X. G. Gong and Q. Q. Zheng, *Phys. Rev. B* **52**, 4756 (1995); Q. Sun, Q. Wang, P. Jena, B. K. Rao, and Y. Kawazoe, *Phys. Rev. Lett.* **90**, 135503 (2003).
- ⁸M. Ohara, Y. Nakamura, Y. Negishi, K. Miyajima, A. Nakajima, and K. Kaya, *J. Phys. Chem. A* **106**, 4498 (2002).
- ⁹H. Prinzbach, A. Weiler, P. Landenberger, F. Wahl, J. Wörth, L. T. Scott, M. Gelmont, D. Olevano, and B. V. Issendorff, *Nature (London)* **407**, 60 (2000).
- ¹⁰L. Mitas, J. C. Grossman, I. Stich, and J. Tobik, *Phys. Rev. Lett.* **84**, 1479 (2000).
- ¹¹K.-M. Ho, A. A. Shvartsburg, B. Pan, Z.-Y. Lu, C.-Z. Wang, J. G. Wacker, J. L. Fye, and M. F. Jarrold, *Nature (London)* **392**, 582 (1998).
- ¹²K. Fuke, K. Tsukamoto, F. Misaizu, and M. Sanekata, *J. Chem. Phys.* **99**, 7807 (1993).
- ¹³U. Röthlisberger, W. Andreoni, and M. Parrinello, *Phys. Rev. Lett.* **72**, 665 (1994).
- ¹⁴V. Kumar and Y. Kawazoe, *Phys. Rev. Lett.* **87**, 045503 (2001); **91**, 199901(E) (2003).
- ¹⁵H. Hiura, T. Miyazaki, and T. Kanayama, *Phys. Rev. Lett.* **86**, 1733 (2001); V. Kumar and Y. Kawazoe, *Phys. Rev. B* **65**, 073404 (2002).
- ¹⁶V. Kumar, *Eur. Phys. J. D* **24**, 227 (2003).
- ¹⁷M. Ohara, K. Koyasu, A. Nakajima, and K. Kaya, *Chem. Phys. Lett.* **371**, 490 (2003).
- ¹⁸A. Nakajima, results presented in the ISSPIC 12 Conference, Nanjing, 2004 (unpublished).
- ¹⁹Q. Sun, Q. Wang, T. M. Briere, V. Kumar, Y. Kawazoe, and P. Jena, *Phys. Rev. B* **65**, 235417 (2002).
- ²⁰T. Nagano, K. Tsumuraya, H. Eguchi, and D. J. Singh, *Phys. Rev. B* **64**, 155403 (2001).
- ²¹F. A. Cotton, G. Wilkinson, C. A. Murillo, and M. Bochmann, *Advanced Inorganic Chemistry*, 6th ed. (Wiley, New York, 1999).
- ²²G. Kresse and D. Joubert, *Phys. Rev. B* **59**, 1758 (1999).
- ²³P. Blöchl, *Phys. Rev. B* **50**, 17953 (1994).
- ²⁴J. P. Perdew, in *Electronic Structure of Solids '91*, edited by P. Ziesche and H. Eschrig (Akademie-Verlag, Berlin, 1991).
- ²⁵W. B. Pearson, *The Crystal Chemistry and The Physics of The Metal Alloys* (Wiley, New York, 1982).
- ²⁶C. J. Smithells, *Metals Reference Book*, 5th ed. (Butterworths, London, 1982), p. 195.
- ²⁷V. Kumar, *Comput. Mater. Sci.* **30**, 260 (2004).
- ²⁸K. Jackson, E. Kaxiras, and M. R. Pederson, *J. Phys. Chem.* **98**, 7805 (1994).

²⁹K. Jackson and B. Nellermore, Chem. Phys. Lett. **254**, 249 (1996).

³⁰We have further done an analysis of the contributions from atomic orbitals to different states by decomposing the charge density contribution from each state into its angular components within a sphere around each ion. The radius of the sphere is taken to be 1.312 Å for Si and 1.588 Å for Th. Significant charge lies outside of these spheres and therefore the analysis of the contributions from different orbitals is only representative. We discuss here only those states of the silicon cage that interact most with the Th atom. Most of the contribution to the $2d$ state (Ref. 31) of the cage comes from the $3p$ orbitals of Si atoms. There are 1.482(0.074) e from $3s$ as compared to 2.164 (2.384) e from $3p$ orbitals and 0.0 (1.02) e from $6d$ orbitals in this state before (after) Th doping. Keeping the normalization in account we conclude that in terms of the atomic orbitals the contribution from $3s$ orbitals of silicon decreases significantly while the contributions from $3p$ orbitals of silicon and $6d$ orbitals of Th increases. The strong bonding can be said to be between the atomic $3p$ orbitals of silicon and the $6d$ orbitals of Th. Contributions to $1s$, $2s$, and $1d$ states of the silicon cage after doping arise predominantly from the $3s$ (0.836 e from $3s$ as compared to 0.054 e from $3p$), $3p$ (0.06 e from $3s$ as compared to 0.652 e from $3p$), and $3s$ orbitals (4.02 e from $3s$ as compared to 0.566 e from $3p$ orbitals) of silicon atoms, respectively. These states are affected only slightly due to Th doping. These contributions from different orbitals are nearly the same as for the undoped Si_{20} cage in which case the values are as follows: for $1s$

cage state 0.858 e from $3s$ and 0.042 e from $3p$; for $2s$ cage state 0.048 e from $3s$ and 0.459 e from $3p$, and for the $1d$ cage state 4.206 e from $3s$ and 0.546 e from $3p$ orbitals of silicon. Similar analysis has been done for the HOMO and the LUMO $1f$ states. The HOMO $1f$ state is not much affected by the Th doping. As discussed in the text the LUMO has stronger interaction with $5f$ orbital of Th atom. The contributions to the $1f$ LUMO states come from $3s$ (0.02 e), $3p$ (1 e) atomic orbitals of Si and $5f$ (1.324 e) atomic orbitals of Th.

³¹It is to be noted that for the undoped Si_{20} cage the HOMO is partially occupied and we used smearing of the states. This leads to the partial occupation of the $2d$ cage states such that approximately 2 more electrons are in the $1f$ cage states. Also because of the smearing the degeneracies of the states are not perfect though the underlying atomic structure has the I_h symmetry which is kept fixed for the empty cage. This leads to some asymmetry in the charge density distribution as it is seen from the $2d$ state shown in Fig. 4(d). Since the charge density is plotted only from one orbital, the overall density is small and therefore the asymmetry in the isosurface is reflected.

³²Doping with Pa(1 μ_B), Pu(4 μ_B), and U(2 μ_B) reduces the icosahedral symmetry to a cubic one and the embedding energies are comparable to that of Th, while in the case of Gd(6 μ_B), Tb(1 μ_B), and Er(1 μ_B) the dodecahedron is distorted and the embedding energies are also significantly reduced. See V. Kumar, A. K. Singh, and Y. Kawazoe (unpublished).

³³F. Pichierri, V. Kumar, and Y. Kawazoe, Chem. Phys. Lett. **383**, 544 (2004).